University of Stavanger

Faculty of Science and Technology

MASTER'S THESIS

Study program/ Specialization: SIGNAL PROCESSING & CYBERNETICS	Spring semester, 2013 Open / ~~Restricted~~ access
Writer: PETER B. KOLSTØ	Peter B. Kolstø (Writer's signature)
Faculty supervisor: PER ANUND AMUNDSEN External supervisor(s): ØYVIND STENSLAND	
Title of thesis: MODELING OF THE VISCOUS EFFECTS IN FLUIDS CONTAINED WITHIN A NARROW PIPE SYSTEM SUPPLIED BY A JET	
Credits (ECTS):	
Key words:	Pages: 48 + enclosure: 11 Stavanger, 17.6.2013 Date/year

Modeling of the viscous effects in fluids contained within a narrow pipe system supplied by a jet

Peter Bergesen Kolstø

June 17, 2013

Contents

List of Figures

Chapter 1

Introduction

1.1 Background

Industrial robots used to spray-paint vehicles use air to place the paint onto the object. The paint is let out at the end of the robot arm, while a stream of air is used to lead the paint towards its desired location. The air supplied to the system comes from a control unit[1] consisting of a high pressure chamber separated from a pipe system by a valve. The valves position as a function of time is preset according to the users desires. Adjustments are then made according to measurements taken of the volume flow through the system. We will regard the ACU as a system consisting of two separate subsystems. The two subsystems are the pipe system supplying the air to the robots tool and the measuring arrangement used to obtain readings of the flow.

We will in this thesis analyze a design where the pipe system is supplied by a valve letting a circular laminar jet into it. The model given here is first and foremost intended to be used to describe the pipe system, but to some lesser degree it also applies to the measuring arrangement. Modeling the inlet as a circular laminar jet is to be considered a suggestion of how to fill the system with fluid. There might be different arrangements that could be used just as well. The reasons for me to chose this particular configuration is that it is mathematically convenient and that it can be assumed to minimizes the effects created as the fluid let in meets the inner walls of the pipe. The straight part of the pipe beyond the valve serves to stabilize the flow before

[1]The control unit in question is referred to as a ACU, which is short for air control unit.

any measurement of it is obtained.

The measurements are done by utilizing a venturi. A venturi consists of two cylindrical pipes with a contracting part in between, which makes up the pipe system. The measurements are obtained by letting some air leak from the pipe system through much narrower pipes on either side of the contracting part of the pipe system to reach a pressure gauge at the end. These narrow pipes makes up the measuring arrangement. The gauge operates by registering the pressure associated with the volume flow through the narrow pipe. The difference between the pressure readings on either side are then used to obtain a measurement of the volume flow through the pipe system. The general description of the system is illustrated in figure 1.1[2]

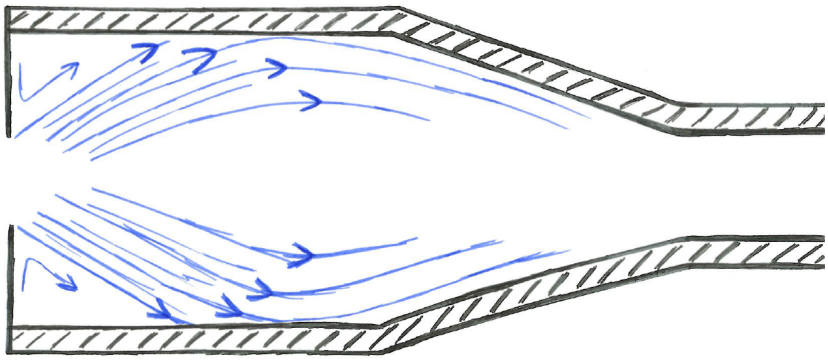

Figure 1.1: General draft of the system under consideration. The streamlines here predict what we intuitively would expect to happen to a jet that is let into the pipe system shown.

1.2 The aim of this thesis

In order to analyze the behavior of the fluid moving through this system we will divide the pipe into three separate sections. Each section will be analyzed in an individual chapter, considering stationary, incompressible flow only. To take into account that the fluid moving through the real system is not stationary, an additional chapter will consider the fluctuation in the

[2]The figure does not show the measuring arrangement as it is not considered a part of the pipe system, but a separate part of the system as a whole.

pressure at the inlet. There will also be separate chapters discussing the effects of compressibility and the effects of a changing pressure gradient in the system.

The first section concerns how the fluid behaves as it emerges from a very small orifice into a large pool of quiescent fluid. The stream will here be treated as a laminar jet, described in cylindrical coordinates. Then as the boundary of the jet reaches the inner walls of the pipe, the second section will aim to describe a turbulent stream contained within a straight, cylindrical pipe. We will include a chapter qualitatively discussing the effects of a changing pressure gradient as the pipe contracts, in order to give a complete description of the pipe system. Then there will be a chapter considering the effects of compressibility. We shall here use dimensional analysis to argue the dominance of the viscous effects over the effects of compressibility. The fluctuation will be analyzed using a known solution for how a harmonically oscillating pressure disturbance propagates through a flow in a pipe. This solution will be elaborated and expanded to include pressure disturbances in the form of a step and an impulse distribution as well.

This thesis will combine elements from both applied physics and electro engineering in an attempt to describe a model of the pipe system and to analyze the valve and the method used for measuring the stream. We will therefore not present a pure mathematical model, but also include some qualitative considerations and notation used in electro engineering. It is my intention to make somewhat complicated mathematical considerations available and easy to apply to practical engineering.

Chapter 2

Cylindrical Laminar Jet

2.1 Background

The mathematical description of a narrow jet of high speed fluid emerging from a small orifice, i.e a laminar jet[1], is derived by using the same assumptions as for a laminar boundary layer. The important facts under this consideration is that the pressure across the jet can not vary to a large extent, and thus, must be approximately the same as the pressure in the surrounding fluid, and that the viscous forces in the direction of motion will be much smaller than those in the radial direction.

Disregarding gravity, as the jet is presumed to move horizontally, and flow in the azimuthal direction; the Navier-Stokes equation for a jet in Cartesian coordinates is reduced to

$$u\frac{\partial u}{\partial x} + v\frac{\partial u}{\partial y} = \frac{1}{\rho}\frac{\partial p_0}{\partial z} + \nu\frac{\partial^2 u}{\partial y^2}. \tag{2.1}$$

This equation in conjunction with the continuum equation

$$\frac{\partial u}{\partial x} + \frac{\partial v}{\partial y} = 0, \tag{2.2}$$

describes the motion of a two-dimensional high speed jet in Cartesian coordinates. Here u and v represents the velocities and x, y and z the spacial

[1]The material in this subsection is found in [2] Pijush K. Kundu, Ira M. Cohen and David R. Dowling 'Fluid Mechanics', unless otherwise stated

coordinates. The density of the fluid is written ρ and the dynamical viscosity is written ν. The solution to this problem is well know and valid for a stationary, incompressible, two-dimensional, laminar, high speed jet, described in Cartesian coordinates that emerges from a narrow slit into a pool of quiescent fluid.

2.2 Exact Solution

We will now proceed by considering a laminar jet of momentum flux J that emerges from a small circular orifice into a large pool of stationary viscous fluid at $z = 0$, as shown in the figure 2.1.

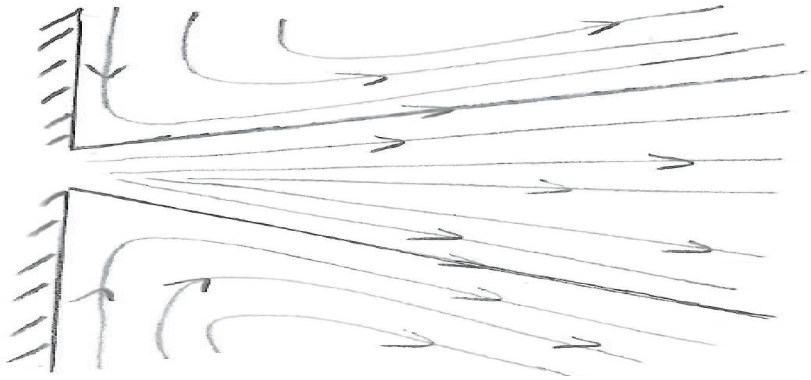

Figure 2.1: A simple sketch of a jet emerging from a small orifice into a large pool of quiescent fluid. The thick lines starting at the orifice serves to illustrate how we might perceive the edge of the jet.

In cylindrical coordinates (2.1) and (2.2) is written respectively[2]

$$w\frac{\partial w}{\partial Z} + U_R\frac{\partial w}{\partial R} = -\frac{1}{\rho}\frac{\partial p_0}{\partial Z} + \frac{\nu}{R}\frac{\partial}{\partial R}\left(R\frac{\partial w}{\partial R}\right) \tag{2.3}$$

and

$$\frac{1}{R}\frac{\partial (RU_R)}{\partial R} + \frac{\partial w}{\partial Z} = 0, \tag{2.4}$$

where Z is the axial coordinate, w is the axial velocity, R is the radial coordinate and U_R is the radial velocity.

[2]See exercise 9.27 in [2] Pijush K. Kundu, Ira M. Cohen and David R. Dowling 'Fluid Mechanics'

Utilizing the continuum equation we seek a similarity solution[3] for the stream function $\Psi(\eta)$. We note that as we utilize the continuum equation we are assuming that there is no fluid entering or leaving the system. This is of course unphysical as we here are considering a jet suppling fluid to large quiescent pool, but we do this in an attempt to simplify the model. The error resulting from this simplification will be analyzed in more detail at the end of this chapter.

$$\Psi = c_1 R g(\eta), \quad \text{where} \quad \eta = (R/Z). \tag{2.5}$$

The axial and radial velocity are found from the stream function as

$$w(\eta) \equiv \left(\frac{1}{R}\right)\frac{\partial \Psi}{\partial R} = (c_1/Z)\Big((1/\eta)g(\eta) + g'(\eta)\Big) \tag{2.6}$$

and

$$U_R(\eta) \equiv -\Big(\frac{1}{R}\Big)\frac{\partial \Psi}{\partial Z} = (c_1/Z)\eta g'(\eta). \tag{2.7}$$

We now define

$$f(\eta) \equiv \Big((1/\eta)g(\eta) + g'(\eta)\Big), \tag{2.8}$$

which gives us

$$\eta f(\eta) = \frac{\partial}{\partial \eta}\Big(\eta g(\eta)\Big) \Rightarrow g(\eta) = \frac{1}{\eta}\int^{\eta} \eta f(\eta) d\eta \tag{2.9}$$

and

$$g'(\eta) = -\Big(\frac{1}{\eta^2}\Big)\int^{\eta} \eta f(\eta) d\eta + f(\eta). \tag{2.10}$$

Substitution of (2.9) and (2.10) into (2.6) and (2.7) enables us to express both the axial and radial velocities as a function of $f(\eta)$ respectively as

$$w(\eta) = \Big(\frac{c_1}{Z}\Big) f(\eta) \tag{2.11}$$

and

$$U_R(\eta) = \Big(\frac{c_1}{Z}\Big)\Big(\eta f(\eta) - \big(\frac{1}{\eta}\big)\int^{\eta} \eta f(\eta) d\eta\Big). \tag{2.12}$$

It is clear from dimensional analysis that since η is a dimensionless variable, c_1 must have the dimension L^2/T in order for (2.11) and (2.12) to have

[3]We here refer to [1] D. J. Tritton 'Physical Fluid Dynamics'

dimension L/T . Thus, we expect that c_1 must be the kinematic viscosity of the fluid. As such, we will further on use $c_1 = \nu$, which enables us to rewrite (2.11) and (2.12) respectively as

$$w(\eta) = \Big(\frac{\nu}{Z}\Big) f(\eta) \tag{2.13}$$

and

$$U_R(\eta) = \Big(\frac{\nu}{Z}\Big)\Big(\eta f(\eta) - (\frac{1}{\eta})\int^{\eta} \eta f(\eta) d\eta\Big). \tag{2.14}$$

The terms in (2.3) is found as

$$\frac{\partial w}{\partial z} = -\Big(\frac{\nu}{z^2}\Big)\frac{\partial}{\partial \eta}\Big(\eta f(\eta)\Big),$$

$$\frac{\partial w}{\partial R} = \Big(\frac{\nu}{z^2}\Big) f'(\eta)$$

and

$$\frac{\partial}{\partial R}\Big(R\frac{\partial w}{\partial R}\Big) = \Big(\frac{\nu}{z^2}\Big)\frac{\partial}{\partial \eta}\Big(\eta f'(\eta)\Big).$$

As the fluid surrounding the jet is said to be quiescent we disregard the pressure gradient

$$\frac{\partial p_0}{\partial z} \approx 0.$$

Substituted into (2.3) the Navier-Stoke equation for a cylindrical jet reduces to

$$f'(\eta) + \eta f''(\eta) + \eta f(\eta)^2 + f'(\eta)\int^{\eta} \eta f(\eta) d\eta = 0. \tag{2.15}$$

In order to solve this, we notice that

$$f'(\eta) + \eta f''(\eta) = \frac{\partial}{\partial \eta}\big(\eta f'(\eta)\big)$$

and that

$$\eta f(\eta)^2 + f'(\eta)\int^{\eta} \eta f(\eta) d\eta = \frac{\partial}{\partial \eta} f(\eta)\int^{\eta} \eta f(\eta) d\eta.$$

This further reduces (2.15) to

$$\eta f'(\eta) + f(\eta)\int^{\eta} \eta f(\eta) d\eta = 0. \tag{2.16}$$

In order to solve eq. (2.16) we introduce

$$F(\eta) \equiv \int^{\eta} \eta f(\eta) d\eta. \tag{2.17}$$

The first and second derivative of $F(\eta)$ are respectively

$$F'(\eta) = \eta f(\eta) \tag{2.18}$$

and

$$F''(\eta) = f(\eta) + \eta f'(\eta). \tag{2.19}$$

Substitution of eq. 2.17, eq. 2.18 and eq. 2.19 into (2.16) yields

$$\eta F''(\eta) + F'(\eta)\big(F(\eta) - 1\big) = 0. \tag{2.20}$$

Preceding to solve this we first notice that

$$F'(\eta)\big(F(\eta) - 1\big) = \frac{1}{2}\frac{\partial}{\partial \eta}\big(F(\eta) - 1\big)^2$$

and that

$$\eta F''(\eta) = \frac{\partial}{\partial \eta}\big(\eta F'(\eta)\big) - F'(\eta).$$

.

This produces

$$\frac{\partial}{\partial \eta}\big(\eta F'(\eta)\big) - F'(\eta) + \frac{1}{2}\frac{\partial}{\partial \eta}\big(F(\eta) - 1\big)^2 = 0 \Leftrightarrow$$

$$\eta F'(\eta) - F(\eta) + \frac{1}{2}\big(F(\eta) - 1\big)^2 = K_1. \tag{2.21}$$

We choose the value of K_1 in such a manner that $F(0) = 0$. The value of K_1 can then be determined as follows

$$K_1 = \eta F'(\eta) - F(\eta) + \frac{1}{2}\big(F(\eta) - 1\big)^2\Big|_{\eta=0} = \frac{1}{2}.$$

Now we can precede to solve (2.21) with $K_1 = 1/2$

$$\eta F'(\eta) - F(\eta) + \frac{1}{2}\big(F(\eta) - 1\big)^2 = \frac{1}{2}.$$

This yields

$$2\eta\frac{\partial F}{\partial \eta} = F(\eta)\big(4 - F(\eta)\big).$$

Integrating this and utilizing that $F(\eta) \to 0$ for $y \to 0$, we find

$$\ln(\eta^2) = \ln\left|\frac{F(\eta)}{4 - F(\eta)}\right| + K_2,$$

which yields

$$F(\eta) = \frac{4K_2\eta^2}{K_2\eta^2 + 1}. \tag{2.22}$$

By redefining $g(\eta)$, found in eq. 2.5, we can chose that $K_2 = 1$, thus we have

$$F(\eta) = \frac{4\eta^2}{\eta^2 + 1}. \tag{2.23}$$

Differentiating this we find an expression for $f(\eta)$

$$f(\eta) = \frac{8}{(\eta^2 + 1)^2}. \tag{2.24}$$

The solution found in eq. 2.24 determines the characteristics of the jet. Further on we will derive the stream function, the radial and axial velocity and the momentum flux of the jet from this function.

2.3 Analysis

2.3.1 The stream function

Substituting (2.24) into (2.9) and further substitution of this into (2.5) with $c_1 = \nu$, gives us the following expression for the stream function of the jet under consideration as we substitute R/Z for η[4]:

$$\Psi(\eta) = \nu R g(\eta) = \nu\Big(\frac{R}{\eta}\Big)\int^{\eta} \eta f(\eta) d\eta$$

[4]We consider Ψ a function of η only for constant ν and R, and use the same consideration for other functions derived from the stream function during this chapter i.e. the functions for the axial and radial velocities and for the momentum flux.

$$= -\nu\Big(\frac{4R}{\eta}\Big)\Big(\frac{1}{\eta^2+1}\Big) = -\nu\frac{4Z}{R^2/Z^2+1} = -\nu\frac{4Z^3}{R^2+Z^2}. \tag{2.25}$$

The plot of eq. (2.25), shown in figure2.2[5], gives some insight into the behavior of the motion of the jet as it emerges from the orifice at $Z = 0$. Here we can follow the innermost lines and observe how the jet expands as it moves along its axis of motion. The outer contours nevertheless deviate from what we expect, as they give the impression that fluid is emerging from every point along the radial axis at $Z = 0$. This of course is not the case in the real system under consideration, as the fluid is entering the system from a small orifice at the center of the pipe. The error arises from the fact that we have not presumed the continuum equation to be valid. As such, the solution we have arrived at in (2.24) necessarily breaks down as we approach $Z = 0$. Further down the axis of motion the outer contours resemble that of fluid being entrained onto the jet, and is what we might expect intuitively. Figure 2.3 illustrates this expected behavior, and we note how it deviates from figure 2.2.

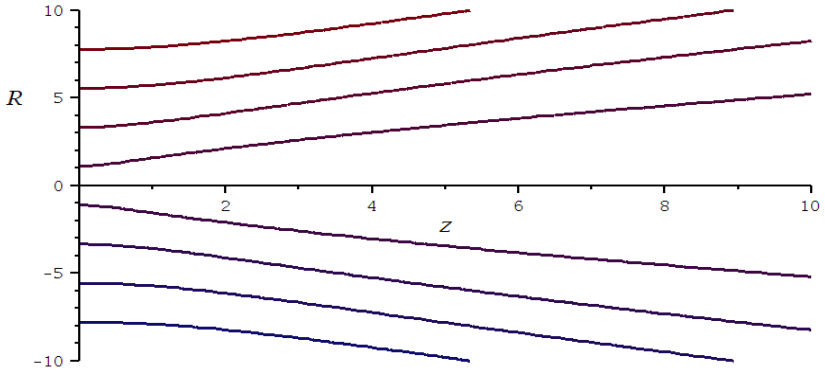

Figure 2.2: Plot of the stream function for the cylindrical jet given in eq. 2.25. It should be noted that we have disregarded the viscosity.

[5]We here note that there might have been made some mistake concerning the plot of the stream function. We will later in this chapter see that the radial velocity approaches infinity and the axial velocity approaches zero in the limit $Z \to 0$. This is not what is shown in figure 2.2. Even so the axial and radial velocities, which are derived from the stream function, seems to agree with our intuition. As such, the seemingly erroneous plot of the stream function might be the result of a technicality in the program used. Nevertheless we see from eq. 2.25 that $\Psi(\eta)$ does approach zero in the limit $Z \to 0$, where we would expect the stream function and radial velocity to yield the same value i.e. infinity, as we at this location surely must have $w = 0$.

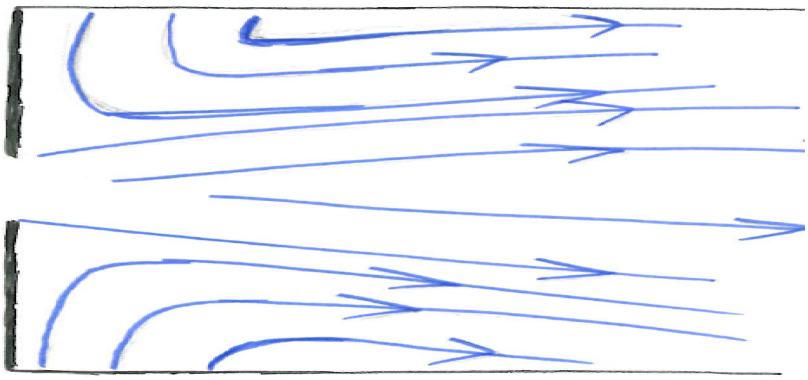

Figure 2.3: Illustration of how we would expect the stream function of a cylindrical jet to behave. We note how the surrounding fluid is being entrained onto the jet .

2.3.2 The radial velocity

Substituting (2.24) into (2.14) yields and expression for the radial velocity as a function of η.

$$U_R(\eta) = \left(\frac{\nu}{Z}\right)\left(\eta f(\eta) - \left(\frac{1}{\eta}\right)\int^{\eta} \eta f(\eta) d\eta\right) = -\left(\frac{\nu}{Z}\right)\frac{4(\eta^2-1)}{(\eta^2+1)^2} \tag{2.26}$$

From eq (2.26) it is seen that

$$\begin{aligned} U_R > 0 \ \text{ for } \ \eta < 1, \\ U_R = 0 \ \text{ for } \ \eta = 1, \\ U_R < 0 \ \text{ for } \ \eta > 1. \end{aligned} \tag{2.27}$$

The result for $\eta < 1$ is in agreement with our intuition as we expect the radial velocity to be positive, but decreasing as we move along the radial coordinate away from the center of the jet. Then $U_R = 0$ is reached as $\eta = 1 \Leftrightarrow Z = R$. For $\eta > 1$ we find the radial velocity to be directed towards the center of the jet. This might seem strange, but can be explained as the velocity of the surrounding fluid being entrained onto the jet.

The error previously discussed, that arises from the fact that we are utilizing the continuum equation in a model of a jet results in a behavior of the radial velocity in the model that deviates from what we are expecting. This is shown in figure 2.4, which illustrates a strange behavior in the radial

velocity as $Z \to 0$. It might be presumed that a correction made in the initial assumption of the stream function might mend this, but this will not be pursued further in this thesis. It should be noted that figure 2.4 is plotted without the scaling (ν/Z). This means that the actual behavior of the radial velocity is to approach infinity in the limit $Z \to 0$, which again shows that the model is unphysical and breaks down as we approach $Z = 0$.

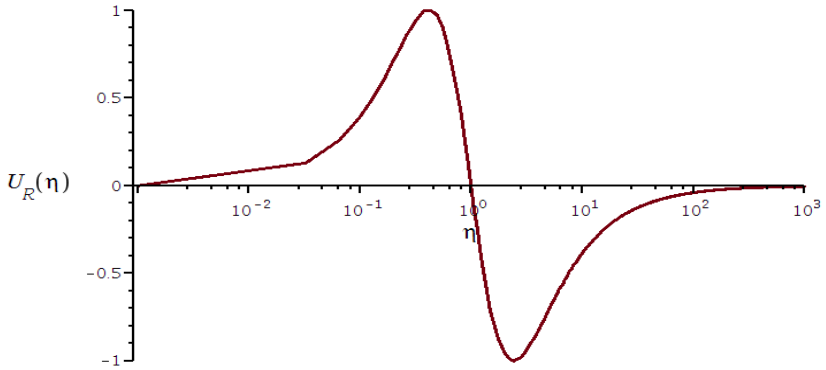

Figure 2.4: A logarithmic plot of the radial velocity for a cylindrical jet. We note the deviating behavior close to $Z = 0$.

In the radial direction we expect that the model of the radial velocity will prove the best results for $\eta < 1$, but even for values of $\eta > 1$ the model might give somewhat accurate description of the behavior of the fluid in this part of the pipe system. In the axial direction we will presume that the model of the radial velocity will improve some distance Z_1 downstream away from the orifice. We assume that this value of Z_1 would at least depend on the diameter D of the orifice, and that these values should be of the same order of magnitude.

2.3.3 The axial velocity

Substitution of (2.24) into (2.13) yields an expression for the velocity in the direction of motion for the jet

$$w(\eta) = \left(\frac{\nu}{Z}\right) f(\eta) = \left(\frac{\nu}{Z}\right)\left(\frac{8}{(\eta^2+1)^2}\right). \tag{2.28}$$

From (2.28) it is clear that the axial velocity falls asymptotically as a fourth power of η. This makes for a jet with a very sharp velocity profile as is

illustrated i figure 2.5. As for the radial velocity, we expect the model for the axial velocity to yield the most accurate results for $\eta < 1$ and some distance Z_1 downstream away from the orifice. We might presume that the model will yield better results for the axial velocity than it will for the radial velocity.

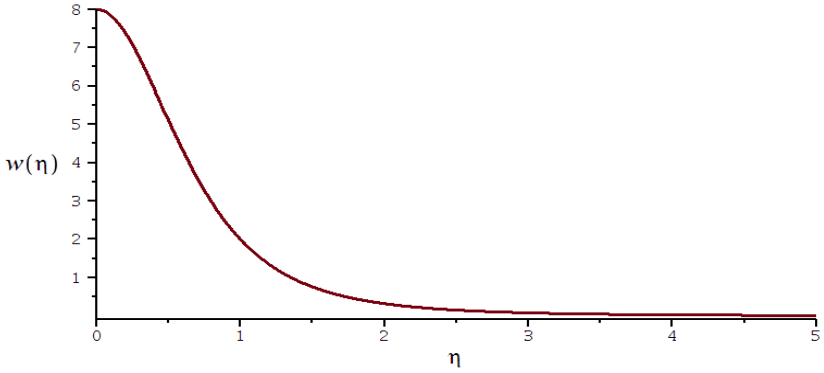

Figure 2.5: The axial velocity of a cylindrical jet. Here plotted without the scaling factor (ν/Z).

2.3.4 Momentum Flux

The momentum flux for a free laminar jet in cylindrical coordinates is given by the expression

$$J = 2\pi\rho \int^{R} w(R,z)^2 R dR. \tag{2.29}$$

As we substitute (2.28) into (2.29) we can express the momentum flux of the jet under consideration as

$$J = \frac{128\pi\rho\nu^2}{Z^2} \int^{\eta} \frac{\eta}{(\eta^2+1)^4} d\eta. \tag{2.30}$$

We have

$$\int^{\eta} \frac{\eta}{(\eta^2+1)^4} d\eta = -\left(\frac{1}{6}\right) \frac{1}{(\eta^2+1)^3} + B. \tag{2.31}$$

The constant B be can be found from the fact that the the momentum flux of the jet must be constant for a free jet. Integrating (2.31) from zero to infinity gives us $B = 1/6$. Form this we find the final expression for the

momentum flux to be:

$$J = \frac{128\pi\rho\nu^2}{Z^2}\left(\frac{1}{6} - \frac{1}{6(\eta^2+1)^3}\right). \tag{2.32}$$

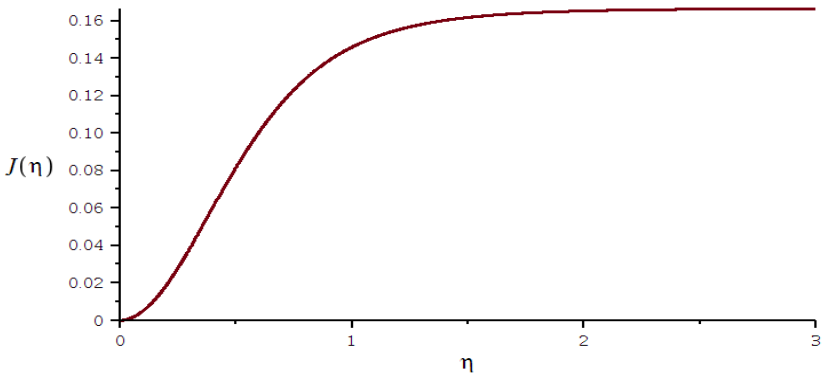

Figure 2.6: The momentum flux of a cylindrical jet, here plotted without the scaling $128\pi\rho\nu^2/Z^2$.

It is seen from eq. (2.32) that the momentum flux falls as η to the sixth power. This is shown in figure 2.6 where the momentum flux converges very rapidly as η grows. As such, most of the momentum flux of the jet is contained within $\eta < 1$. This might be seen as support of the assumption that the model of the jet will generally prove the best results for $\eta < 1$.

We have not included any calculation of the volume flow for the laminar jet. The reason for this is that the bulk of fluid that makes up the jet increases as more of the surrounding fluid is entrained onto the jet as it moves along the axis of motion. As such the momentum flux of the jet is the appropriate estimate for the size of the jet, as it remains the same for all values of Z.

2.4 Discussion

6

[6]We will in this subsection frequently refer to [1] D.J. Tritton 'Fluid Dynamics'

2.4.1 The edge of the jet

During operation the axial velocity is positive and non-zero inside the pipe system for all values of R and Z. As such there will be a build up of a boundary layer along the entire pipe. Even so the axial velocity decreases rapidly for an increasing value of η, and as such it might be appropriate to define a value which we can expect a build up of a significant boundary layer on the inside of the pipe system containing the jet. We have previously argued that the model of the jet will likely prove the best results for $\eta < 1$. From eq. (2.26) we have that the radial velocity reaches zero as $\eta = 1$. At this value of η it can be seen from eq. (2.28), that the axial velocity have reduced to one fourth of its maximum. As such, we might use $\eta = 1 \Leftrightarrow R = Z$ as a starting point for an experimental search for an appropriate value of η for which we can define to be the edge of the jet.

We also have that the assumption of a free laminar jet necessarily must be rendered invalid at some point because of the interference of the walls containing it. The error of this approximation will be omitted in this thesis, but having an edge of the jet enables us at least to measure the distance between the wall of the pipe system and what we regard as the jet. By choosing $R = Z$ as the edge of the jet we see that we have defined that jet will propagate in a 45 degree angle in the radial direction as it moves along the axial direction.

2.4.2 The orifice from where the jet emerges

We will now discuss the consequences of utilizing the continuum equation in a model of a jet, and make clear the boundary conditions at the orifice from where the jet emerges.

As we substitute $\eta = R/Z$ into eq. (2.28) and eq. (2.26), we have in the limit $Z \to 0$ respectively

$$w(R,Z) = \lim_{Z\to 0}\Big(\frac{\nu}{Z}\Big)\Big(\frac{8}{((R/Z)^2+1)^2}\Big) = \lim_{Z\to 0}\Big(\frac{8\nu Z^3}{((R^2+Z^2)^2}\Big) = 0 \quad (2.33)$$

and

$$U_R(R,Z) = \lim_{Z\to 0} -\Big(\frac{4\nu}{Z}\Big)\frac{((R/Z)^2-1)}{((R/Z)^2+1)^2} = \lim_{Z\to 0} -4\nu Z\frac{(R^2-Z^2)}{(R^2+Z^2)^2} = 0. \quad (2.34)$$

From eq. (2.33) and eq. (2.34) we see that there is no fluid entering into the system at $Z = 0$. The model therefore predicts that the jet is given momentum by a source emerging from an infinite small opening at $(Z = 0, R = 0)$ that is not providing any mass to the system. This is of course unphysical, but it greatly simplifies the model. How the jet is given mass can be seen from dividing eq. (2.34) by eq. (2.33)

$$\frac{U_R}{w} = \frac{-\left(\frac{4\nu}{Z}\right)\frac{(\eta^2-1)}{(\eta^2+1)^2}}{\left(\frac{\nu}{Z}\right)\frac{8}{(\eta^2+1)^2}} = -\frac{1}{2}(\eta^2 - 1) = \frac{1}{2}(1 - \frac{R^2}{Z^2}). \tag{2.35}$$

Eq. (2.35) shows that as we approach $Z = 0$ the radial velocity grows towards infinity for all values of R. As such we find that the jet here is given its mass from fluid being drawn from the surroundings onto the the center just beyond $Z = 0$.

2.4.3 Stability

The velocity profile of a jet as a turning point i.e. a non-zero value for its second derivative. We know from experimental data that flows of this kind are much more prone to instabilities than flows without. Hence, we presume that the jet will most likely dissolve close to the point from where it emerges. Nevertheless the surrounding walls of the pipe will serve to stabilize the jet, so that we might presume a jet structure of the flow for some length of the system. We will assume that the flow retains its characteristics as a jet at least long enough for its edge to reach the inner walls of the pipe i.e. $\eta = 1 \Leftrightarrow R = Z$.

2.4.4 The effects of fluctuations in the pressure gradient on the jet

We presume that the effects that fluctuations of the pressure gradient in the flow will have upon both the jet and the surrounding fluid will be significant. An increase of the velocity of the flow will lead to a higher degree of stability in the jet, while a decrease will make it more unstable. What effects rapid fluctuations will have on the flow near the valve will not be pursued further in this thesis. Nevertheless we will presume that the fluctuations will cause

a larger degree of instabilities in the jet, and that this might cause it to undergo the inevitable transition from a structured laminar jet to a regular turbulent flow at a faster rate than a stationary jet.

2.4.5 The transition from jet to regular turbulent flow

We presume that as the jet breaks down because of the interference with the wall or because of instabilities within the jet itself the flow will undergo a sudden transition from a laminar jet to a regular turbulent flow. We will presume it to be crucial that this transition has taken place i.e. that the flow has been stabilized enough for it to be described as a regular turbulent flow, before it reaches any point where measurements of it are obtained. It should be noted that it would possible prove very hard to obtain proper readings of the flow as it undergoes the transition, and that this might also prove right as we regard the jet as well.

Chapter 3

Turbulent Flow Near a Wall

3.1 Background

In this chapter we will presume the pipe to be filled with a more or less homogeneous turbulent flow. The high velocity of the flow required to make the assumptions for the jet valid, results in a high Reynolds number in the flow following the jet. As such we can not hope to find an analytic solution to the Navier-Stokes equation for the behavior of the flow. Instead we will rely on the analysis made by von Karman in his deduction of the behavior of a turbulent shear flow near a wall in order to describe the stream in this part of the system[1].

3.2 The analysis made by von Karman

The boundary layer of a turbulent flow is divided into an inner laminar and an outer turbulent zone. As the velocity of the mean flow U can only be a function of the flow near the wall u_τ, the kinematic viscosity ν and the distance from the wall y, it is given from dimensional analysis that the profile of turbulent two-dimensional wall flows is

$$\frac{U}{u_\tau} = \frac{1}{K}\left[ln\left(\frac{yu_\tau}{\nu}\right) + A\right], \tag{3.1}$$

[1]The material in this section here refer to [1] D.J. Tritton 'Fluid dynamics', unless otherwise stated

where K is the von Karman constant and A is an arbitrary constant of integration. Experimentally the ratio U/u_τ is found to be in the range 0.035 to 0.05, and is found to depend rather weakly on the Reynolds number. K is likewise experimentally found to be approximately equal to 0.40.

The logarithmic velocity profile for the turbulent part of a boundary layer, described in (3.1), proves the best results when $30 < yu_\tau/\mu < 200$, where yu_τ/μ scales the thickness of the turbulent boundary layer. Below this we expect a linear velocity profile for the laminar part of the boundary layer. Above the boundary layer the profile will depend on the flow as a whole. From this we will presume that for any velocity high enough to produce a turbulent flow, we will have a very thin turbulent boundary layer and an even thinner laminar layer underneath. The profile of the flow as a whole and the profile of the laminar sublayer will deviate from the profile described in this section. Nevertheless we shall presume that this logarithmic profile will be a valid approximation in these region, but that it will agree the most with experimental results in the range given above.

3.3 Turbulent motion near a cylindrical wall

To be able to apply (3.1) to a flow through a cylindrical pipe we will make the following assumption that $y \approx a - r^2$. We can do this as we already have assumed that the thickness of the boundary layer is very small. Substitution of this assumption into (3.1) gives the equation

$$U(r) = \frac{u_\tau}{K}\left[ln\left(\frac{a-r}{a}\right) + ln\left(\frac{au_\tau}{\nu}\right) + A\right]. \tag{3.2}$$

In the center of the pipe we find the maximum velocity of the flow through this part of the system to be

$$U_m = U(0) = \frac{u_\tau}{K}\left[ln\left(\frac{au_\tau}{\nu}\right) + A\right]. \tag{3.3}$$

Using eq. 3.3 we can now rewrite eq. 3.2 as

$$U(r) = U_m + \frac{u_\tau}{K}\left[ln\left(1 - \frac{r}{a}\right)\right], \tag{3.4}$$

[2]We here refer to verbal information given by Per Amund Amundsen'

which gives us the velocity profile of a turbulent flow through a pipe. Furthermore we can use the experimental data given above to rewrite eq. 3.4 as

$$U(r) = U_m\left(1 + \frac{1}{10}\Big(ln(1-b)\Big)\right), \tag{3.5}$$

where we have presumed the ratio u_{tau}/U_m to be 0.04 and K to be 0.4. We have also introduced b as the ratio between the radial coordinate r and the maximum radius of the pipe a for the sake of convenience. From (3.5) it is clear that the shape of the velocity profile is given by the ratio $b = r/a$, and that U_m merely serves to scale this profile.

3.4 The thickness of the boundary layer

As expected we find that the part of the flow where the velocity deviates to a large degree from the mean velocity of the flow is contained only very close to the wall. This is clear from figure 3.1, which shows the velocity profile of a turbulent flow through a cylindrical pipe. We note the square profile of the turbulent flow through the pipe system under consideration in contrast to the gentle slope of the Possuille-Hagen flow. We also note that we have plotted the logarithmic profile of the turbulent boundary layer in the entire range of the pipes radius.

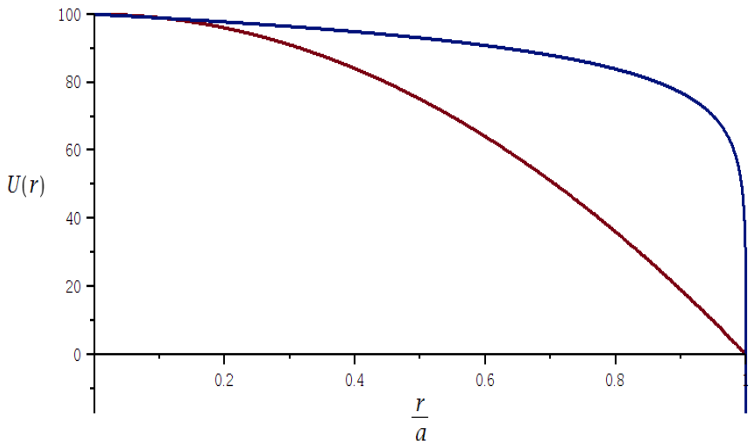

Figure 3.1: The velocity profile of a turbulent flow through a pipe for (blue line). Plotted in contrast to the Possuille-Hagen profile (red line).

A convenient way of measuring the thickness of the boundary layer would be to define it to be at the value of r where the derivative of $U(r)$ is equal to one. Another way would be to define it to be where the velocity is less than 99% of the mean velocity. With the first definition we find it to be $b = 0.9999498$, and with the second we find it to be $b = 0.9999546$, both for $U_m = 100$ m/s. In either case we have such a thin boundary layer that it can be neglected for any velocity of practical interest in the real system. Hence, we can conclude that we may disregard the velocity profile given in this chapter and only consider the mean velocity as we describe the flow in this section of the pipe system. We note that even as we might discard the thickness of the boundary layer we must still take into account how the non-slip condition affects the velocity profile in the pipe. We can therefore not utilize the maximum velocity in calculations of the volume flow, but must instead use the mean average velocity. The reason for this can be seen from figure 3.1, where we note how the velocity increases for a decreasing radial coordinate outside the boundary layer as well as within. The boundary layer also sustain the turbulence in the pipe system by transporting vorticity into the main stream, and then there are the effects of separation and friction.

3.5 Volume flow

Even as the flow in this section of the pipe system can be pretty accurately described by its mean velocity we note that there will exist fluctuations of the velocity atop the mean velocity in a turbulent flow. These fluctuations might be significant considering the very turbulent nature of the flow in the real system.

The solution for the volume flow as we apply eq. 3.5 along the entire radius of the pipe is given as

$$Q = 2\pi \int_0^a u(r) r dr = 2\pi U_m \int_0^a r\left(1 + \frac{1}{10}\Big[ln\Big(1 - \frac{r}{a}\Big)\Big]\right) dr$$

,

$$= 2\pi U_m \left(\int_0^a r dr + \frac{1}{10} \int_0^a r\Big[ln\Big(1 - \frac{r}{a}\Big)\Big] dr \right) = 2\pi U_m \left(\frac{1}{2}a^2 - \frac{3}{40}a^2 \right)$$

$$= 2\pi a^2 U_m (0.425) = 0.85\pi a^2 U_m \tag{3.6}$$

From eq. (3.6) we see that even as the boundary layer is very thin the volume flow is reduced to 42.5% of what the flow would have been if the maximum velocity would have been present all over the radial axis.

3.6 Discussion

The assumption that $y \approx a - r$ made in the calculation of (3.4) leads to a result that deviates some from what we expect from a physical point of view. We would expect that the derivative of the radial velocity with respect to the radial coordinate should be zero at the center of the pipe. But as can be seen the derivative of (3.4) at $r = 0$ yields

$$\left.\frac{dU(r)}{dr}\right|_{r=0} = \frac{u_\tau}{aK} \neq 0. \tag{3.7}$$

This results in a small deviation from what we would expect in the velocity profile around the center of the pipe. The error here will in most cases be acceptable as the model yields a velocity that is accurate in the mean. As such, we keep eq. (3.6) as an appropriate approximation of the volume flow.

Chapter 4

Changing Pressure Gradient

To be able to give a complete description of the pipe system we will now turn our attention to the contracting part of it and qualitatively consider the effects the gradually decreasing diameter of the pipe system will have on the flow described in the previous chapter. This is not to be considered a part of the mathematical model of the system, but serves to clarify some aspects associated with the change of conditions in a boundary layer. We do this in an attempt to wheel this thesis in the direction of practical engineering and further design of the system.

In the case of a stationary flow we will have a favorable pressure gradient at the contracting part of the pipe i.e.

$$\frac{\partial u_0}{\partial x} > 0 \quad \Leftrightarrow \quad \frac{\partial p_0}{\partial x} < 0.$$

First and foremost, a smaller diameter will serve to increase the velocity and decrease the pressure and thus stabilize the flow[1]. As the pressure decreases through the contracting part of the pipe the turbulent boundary layer will become increasingly thinner. At the same time the increase of the Reynolds number will cause the turbulence within the boundary layer to increase. Thus, the portion of the flow producing the turbulence will become smaller even as it produces more turbulence. This turbulence will be transported into the main stream.

The high velocity of the flow under normal operating procedures makes it unlikely that the boundary layer will separate under stationary conditions.

[1]We will in this chapter refer to [1] D. J. Tritton 'Physical Fluid Dynamics'

Even so, we suspect that it will be more likely that the boundary layer will separate at the points where the pipe system starts to and ceases to contract. We will expect that the increase of the instability in the boundary layer at these locations will rely on the smoothness of the transition. If these transitions are not sufficiently smooth there might be areas contained close to the transitions where we might have an adverse pressure gradient, which in turn might cause a separation.

The effects caused by fluctuations will contribute to the conditions for separation of the boundary layer in the pipe system. As the velocity of the flow decreases an adverse pressure gradient is produced in the entire flow. If the decrease of the flow rate lasts long enough for the boundary layer to separate, there would be a significant increase in the transport of turbulence from the boundary layer into the main flow. As a consequence of this increased turbulence the mean velocity in the axial direction will slow down, as energy is needed to maintain the higher degree of random motion of the fluid particles.

Chapter 5

Compressibility

The valve that separates the high pressure chamber and the pipe system is able to take on any range of openings, from complete shutdown, to letting in air moving at sonic speed. We will presumed that the conditions for supersonic velocities are not present in the system[1]. Therefore the maximal velocity of the stream i.e. the local speed of sound, is reached before the valve has fully opened. Depending on the design of the valve the stream might nevertheless reach supersonic velocities as it is let into the pipe system, but we will then presume that the stream will return to sonic conditions through the means of oblique shock waves short after. Typically the velocity of air through the system will range from 40 to $90m/s$ at the widest part and from 150 to $300m/s$ at the narrowest part of the pipe system. From this we have that the flow will reach velocities in the pipe system for which the effect of compressibility will range from noticeable to very significant.

Compressibility becomes a significant effect as the fluid in question reaches velocities of about 30% of the local speed of sound. For velocities below this the results reached by assuming incompressibility deviates from experimental results by less than 20%. The assumption of incompressibility will therefore result in an noticeable error in the real system under consideration, as the fluid used here is air of velocities approaching the local speed of sound. Even so it will be made clear that the time constant of the effects caused by the compressibility of the fluid is much smaller than the time constant of the effects caused by the viscous forces. As such we can reasonably argue a model of the system based on the viscous effects only. There will be effects caused

[1]We will in this chapter refer to [2] Pijush K. Kundu, Ira M. Cohen and David R. Dowling 'Fluid Mechanics'

by compressibility, such as the shock waves created if the flow should pass the local speed of sound and the chocking of fluids moving at sonic velocities, that are not affected by this difference of the time constants, but they will not be pursued further in this thesis.

Using dimensional analysis on the effects caused by compressibility in the pipe system under consideration, we have that the length scale is the distance from the valve to the inlet of the pressure gauge and the velocity scale is the speed of sound. If the medium is air, with a local speed of sound $c \approx 300m/s$ and a length from the inlet to the point of measuring $l \approx 10cm$, we have that the time constant for the compressible effects is of the order $l/c \approx 3 * 10^{-4}sek$. We shall see in chapter 6 that the time scale for the viscous effects are of the order a^2/ν. Using $\nu \approx 1.5 * 10^{-5}m^2/s$ for air under conditions associated with normal operating procedures, and $a \approx 1cm$ being a typical radius for a pipe, the time scale of the viscous effects becomes of the order $a^2/\nu \approx 6sek$. We see that the time scale for the viscous effects will be about 10^4 times larger than what the time scale for the compressible effects are in this case. We presume that the effects of compressibility can be considered linear with regard to the viscous effects. Hence, as we are concerned with the time it takes for the volume flow to adjusts to changes in the pressure of the flow it seems appropriate to neglect the effects of compressibility as we regard how the volume flow adjusts to changes of the pressure in the flow.

Chapter 6

Oscillating Flow

6.1 Background

The problems discussed so far apply to stationary flows only. As the real system under consideration operates with a unsteady flow we will now give some consideration of how to mend this. Provided by Per Amund Amundsen is a solution for how a harmonically oscillating pressure affects the volume flow through a pipe system. This chapter will elaborate and expand that solution to include other types of pressure changes in the flow. This expansion will not be applied to the solution for the laminar jet as it is beyond the scope of this thesis, but it will serve to give a model for how the stream behaves as it is considered to fill an entire straight pipe. As such the solution does not apply to the converging part of the pipe system. We note that the solutions discussed here apply to an laminar flow in a straight pipe, and that the fluid through the real system is both turbulent and contracting. Even so, the solution given in this chapter will give a general overview of the process that illustrates the mechanism of some of the determining variables. These variables would among others be the time constant and the amplification of the process in the pipe system under consideration.

The solutions here will also serve to give a method of improved measurements of the flow as well as describing it. If the measurements of the flow are done by attaching a separate pipe to the pipe system, as is the case we are considering here, then this model will apply to that pipe as well. Even so we note that this model is developed in order to describe oscillating fluid moving through pipes with a diameter a of some magnitude, and that some caution might be called for as it is applied to a very narrow pipe.

6.2 Mathematical considerations

6.2.1 Transformation of the velocity profile

The Navier-Stokes equation in cylindrical coordinates for a time-varying, incompressible, laminar flow in a straight pipe, with no flow in the azimuthal direction and with the gravitational forces disregarded is reduced to

$$\rho\frac{\partial u}{\partial t} = -\frac{\partial p}{\partial z} + \mu\left(\frac{\partial^2 u}{\partial r^2} + \frac{1}{r}\frac{\partial u}{\partial r}\right), \tag{6.1}$$

with the pressure in the pipe system given by[1]

$$p(r,z,t) = p(z,t) = -\frac{\Delta p(t)}{l}z + p_0(t). \tag{6.2}$$

Eq. (6.1) can be solved by the use of Fourier analysis. In order to do so we will transform every term in eq. (6.1) into the frequency domain and then transform the entire equation back to the time domain.

We will here respectively use the following definition for the Fourier and the inverse Fourier transform[2].

$$X(\omega) = \int_{-\infty}^{\infty} x(t)e^{-i\omega t}$$

$$x(t) = \frac{1}{2\pi}\int_{-\infty}^{\infty} X(\omega)e^{i\omega t}. \tag{6.3}$$

From the definition given in (6.3) we have that eq. (6.1) equals

$$\frac{1}{2\pi}\int_{-\infty}^{\infty}\left[-\rho\frac{\partial \tilde{u}}{\partial t} - \frac{\partial \tilde{p}}{\partial z} + \mu\left(\frac{\partial^2 \tilde{u}}{\partial r^2} + \frac{1}{r}\frac{\partial \tilde{u}}{\partial r}\right)\right]e^{i\omega t}d\omega = 0, \tag{6.4}$$

[1] With reference to 'Per Amund Amundsens, unpublished note concerning oscillating flows'

[2] We here refer to [3] B. P. Lathi 'Linear Systems and Signals'.

where $\tilde{u}(r,w)$ and $\tilde{p}(w)$ are the Fourier transform of $u(r,t)$ and $p(t)$ respectively.

The following theorem states that for any function $F(x,y)$[3]

$$\int_{-\infty}^{\infty} F(x,y)e^{i\omega t}d\omega = 0 \ \ \forall \ \ \omega \ \ \text{then} \ \ F(x,y) = 0. \tag{6.5}$$

Now, with reference to theorem (6.5) we see that eq. (6.4) is solved as long as

$$-\rho\frac{\partial\tilde{u}}{\partial t} - \frac{\partial\tilde{p}}{\partial z} + \mu\left(\frac{\partial^2\tilde{u}}{\partial r^2} + \frac{1}{r}\frac{\partial\tilde{u}}{\partial r}\right) = 0. \tag{6.6}$$

Having transformed eq. (6.1) with regard to t only we find the terms in (6.6) to yield

$$\frac{\partial\tilde{u}(\omega,r)}{\partial t} = i\omega\tilde{u}(r,\omega)$$

and

$$\frac{\partial\tilde{p}(\omega)}{\partial z} = -\frac{\tilde{\Delta}p(\omega)}{\mu l},$$

while the last two terms remain unchanged with respect to there derivatives. Substitution of the transformed terms into eq. (6.6) enables us to rewrite it as

$$\frac{\partial^2\tilde{u}}{\partial r^2} + \frac{1}{r}\frac{\partial\tilde{u}}{\partial r} - \frac{i\omega\rho}{\mu}\tilde{u} + \frac{\tilde{\Delta p(\omega)}}{\mu l} = 0. \tag{6.7}$$

Subject to the boundary conditions $u(a) = 0$ and $u(0)$ being finite. The solution of eq. (6.7) is given by

$$\tilde{u}(r,\omega) = \frac{-i\tilde{\Delta}p(\omega)}{\rho\omega l}\left(1 - \frac{J_0\left(r\sqrt{\frac{-i\omega}{\nu}}\right)}{J_0\left(a\sqrt{\frac{-i\omega}{\nu}}\right)}\right), \tag{6.8}$$

where J_0 is a Bessel function of order zero.

The inverse Fourier transform of (6.8) yield the velocity profile in the time domain

$$u(r,t) = \frac{1}{2\pi}\int_{-\infty}^{\infty}\tilde{u}(r,\omega)e^{i\omega t}d\omega. \tag{6.9}$$

[3]We here refer to [4] George Arfken 'Mathematical Methods for Physicists'

It would be convenient to consider the poles contributed by the transform of the function for the pressure separate from the rest of the function in eq. (6.8). As such we define

$$f(\omega) = \frac{1}{\omega}\left(1 - \frac{J_0\big(r\sqrt{\frac{-i\omega}{\nu}}\big)}{J_0\big(a\sqrt{\frac{-i\omega}{\nu}}\big)}\right)e^{i\omega t}. \tag{6.10}$$

We will now use eq. 6.10 to rewrite eq. 6.9

$$u(r,t) = \frac{-i}{2\pi\rho l}\int_{-\infty}^{\infty}\tilde{\Delta p}(\omega)f(\omega)d\omega. \tag{6.11}$$

Eq. (6.11) is a complex function with poles. As such we will solve it by the use of the theorem of residues[4].

$$u(r,t) = 2\pi i\sum_k Res\left[\frac{-i}{2\pi\rho l}\tilde{\Delta p}(\omega)f(\omega),\omega_0\right] = \frac{1}{\rho l}\sum_k Res\Big[\tilde{\Delta p}(\omega)f(\omega),\omega_0\Big], \tag{6.12}$$

where ω_0 are the poles of the functions in question.

The velocity profile can be determined from the sum of the residues contributed by the poles of the function $f(\omega)$ and $\tilde{\Delta p}(\omega)$.

$$u(r,t) = \frac{1}{\rho l}\bigg(\sum_k Res\big[\tilde{\Delta p}(\omega)f(\omega),\omega_k\big] + \sum_m Res\big[\tilde{\Delta p}(\omega)f(\omega),\omega_m\big]\bigg), \tag{6.13}$$

where ω_k and ω_m are the frequencies that yield poles in the function $f(\omega)$ and the transform of the pressure function $\tilde{\Delta p}(\omega)$ respectively.

6.2.2 Closing the contour

We will now proceed to close the contour around the residue in eq. 6.13. The important point then is to ensure that the part of the circle-integral not along the real axis in eq. (6.9) does not contribute to the final value. As we are considering a real system we will only include positive values of the time t. From eq. (6.9) we see that the factor that might approach infinity for an

[4]We here refer to George Arfken 'Mathematical Methods for Physicists'

increasing value of t is $e^{i\omega t}$, with $\omega = x + yi$, we have $e^{ixt}e^{-yt}$, the absolute value of which is $|e^{-yt}|$. It is imperative that $|e^{-yt}| \to 0$ on the part of the circle-integral not along the real axis, from this it is seen that the contour must be taken around the upper half plane. The contour will be encircled in a counterclockwise direction as the integral is taken from $-\infty$ to ∞ along the real axis. To ensure that the integral remains finite we shall therefore only include the poles contributed by the Bessel function and the transform of the pressure functions in the upper half plane. Figure 6.1 serves to illustrate this.

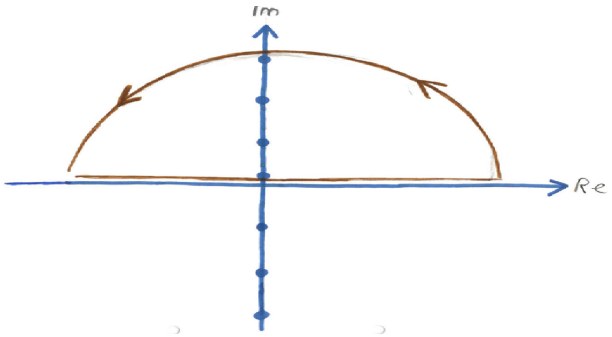

Figure 6.1: The contour enclosing the poles in question. The dots placed symmetrically along the imaginary axis illustrates the first few poles of the Bessel function in eq. 6.8. The lone dot on the positive imaginary axis near the origin, is situated at the location of the pole of the transform of the step function and serves as an example of how poles contributed by the transform of pressure functions are included in the contour.

6.2.3 Transform of pressure functions and distributions

We now turn our attention to the transforms of the pressure distributions and functions[5] in question from the time domain into the frequency domain and locate there poles. We will in this thesis only consider an impulse and a step distribution and a harmonic function[6].

[5]Further on we will refer to both the functions and distributions of the pressure in general we will simply call them functions.

[6]We will in this subsection refer to [3] B. P. Lathi 'Linear Systems and Signals', unless otherwise stated

Even though an impulse and a step distribution are not functions in the classical sense, we have that they can still be transformed into and out of the frequency domain according to Fourier theorem as they here act upon another function. As such they can still be subject to Fourier transform all though they do not satisfy the Dirchlet conditions by themselves[7].

Transform of a harmonic function

We will here represent a harmonic function for the pressure in the time domain $\Delta p \cos(\omega_0 t)$ as the real part of a complex exponential $\Delta p \Re\left[e^{i\omega_0 t}\right]$.[8] The transform into the frequency domain is then given as

$$\Delta p(t) = \Delta p e^{i\omega_0 t} \Leftrightarrow \Delta\tilde{p}(\omega) = \Delta p \int_{-\infty}^{\infty} e^{i\omega_0 t} e^{-i\omega t} dt$$

$$= \Delta p \int_{-\infty}^{\infty} e^{i(\omega-\omega_0)t} dt = \Delta p \delta(\omega - \omega_0) = \frac{\Delta p}{\pi} \lim_{\epsilon \to 0} \frac{\epsilon}{(\omega-\omega_0)^2 + \epsilon^2}^{9}. \quad (6.14)$$

Here we have poles located in both $\omega = \omega_0 - i\epsilon$ and $\omega = \omega_0 + i\epsilon$. Since the contour excludes the lower half plane we will only have contributions from $\omega = \omega_0 + i\epsilon$.

Transform of the impulse distribution

For an impulse distribution in the time domain $\Delta p \delta(t)$ we have from the sampling theorem that the transform into the frequency domain is given as

$$\Delta p(t) = \Delta p \delta(t) \Leftrightarrow$$

$$\Delta\tilde{p}(\omega) = \int_{-\infty}^{\infty} \Delta p \delta(t) e^{-i\omega t} dt = \Delta p. \quad (6.15)$$

It is clear from eq (6.15) that the transform of an impulse function does not contribute any poles in eq (6.13). It can be noted that to represent an impulse distribution in the time domain an equal amount of every possible frequency is needed in the frequency domain.

[7] We here refer to [5] Eugen Butkov 'Mathematical Physics'

[8] Note that we further on will skip the notation $\Re$ for the real part for the sake of convenience. As such we must simply keep in mind that we are always considering real systems and signals during all of this thesis.

[9] We here refer to [7] Frank W. Olver, Danile W. Lozier, Ronald F. Boisvert and Charles W. Clark 'Nist handbook of mathematical functions'

Transform of the step distribution

A step distribution in the time domain $\Delta p\theta(t)$ is represented in the frequency domain as

$$\Delta p(t) = \Delta p\theta(t) \Leftrightarrow$$

$$\Delta\tilde{p}(\omega) = \Delta p \int_0^\infty e^{-i\omega t}dt = \frac{\Delta p}{-i\omega}e^{-i\omega t}\Big|_0^\infty = \frac{\Delta p}{i\omega}. \tag{6.16}$$

In the form of a step distribution we have that the transform of the pressure yields a pole situated at $\omega = i\epsilon$, where ϵ is an arbitrary small number. It might not be entirely clear from eq. 6.48 that the pole should be situated here, but as we consider the inverse transform it is clear that it must be this way. This pole contributes to eq. (6.13)[10].

6.2.4 The poles of the function $f(\omega)$

We will now consider the poles from function $f(\omega)$ described in eq. 6.10 that contributes to the residue described of eq. 6.13 . The Bessel function in the enumerator in eq. 6.10 clearly contributes an infinite number of poles. In addition to this we must also consider whether there is a pole at $\omega = 0$. To see that this is not the case we shall use the Taylor expansion of the Bessel function around $\omega = 0$ considering the two first terms only,

$$J_0(z_i) = J_0(z_i) + J_0'(z_i)(z - z_i) + J_0''(z_i)(z - z_i)^2 + \ldots \Rightarrow$$

$$J_0\big(r\sqrt{\frac{-i\omega}{\nu}}\big) \approx 1 - \frac{\big(r\sqrt{\frac{-i\omega}{\nu}}\big)^2}{4} = 1 + \frac{\frac{ir^2\omega}{\nu}}{4}. \tag{6.17}$$

Having done the same expansion for the enumerator as for the numerator, we substitution eq. (6.17) into eq. (6.10) and find

$$f(0) = \lim_{\omega\to 0}\frac{1}{\omega}\left(1 - \frac{J_0\big(r\sqrt{\frac{-i\omega}{\nu}}\big)}{J_0\big(a\sqrt{\frac{-i\omega}{\nu}}\big)}\right)e^{i\omega t} \approx \lim_{w\to 0}\frac{1}{\omega}\left(1 - \left(\frac{1 + \frac{1}{4}\frac{ir^2\omega}{\nu}}{1 + \frac{1}{4}\frac{ia^2\omega}{\nu}}\right)\right)e^{i\omega t} \tag{6.18}$$

[10]In the following it shall always be assumed that $i\omega$ is shorthand for $\omega - i\epsilon$

As $-1 < \omega < 1$ we can develop a series expansion of the enumerator through the relation

$$\frac{1}{1+x} = 1 - x + x^2 - x^3 + x^4 - \dots. \tag{6.19}$$

Approximating eq. 6.18 by its two first terms, we have

$$\begin{aligned} f(0) &\approx \lim_{\omega\to 0} \frac{1}{\omega}\left(1 - \left(1 + \frac{1}{4}\frac{ir^2\omega}{\nu}\right)\left(1 - \frac{1}{4}\frac{ia^2\omega}{\nu}\right)\right)e^{i\omega t} \\ &= \lim_{\omega\to 0} \frac{1}{\omega}\left(\frac{1}{4}\frac{ir^2\omega}{\nu} - \frac{1}{4}\frac{ia^2\omega}{\nu} + \frac{1}{16}\frac{a^2r^2\omega^2}{\nu^2}\right)e^{i\omega t} \end{aligned} \tag{6.20}$$

As we here are considering only very small values of ω, we will no discard the second order term for w, in eq. 6.20. As such we have that

$$f(0) \approx \frac{1}{\omega}\left(i(a^2 - r^2)\frac{\omega}{4\nu}\right) = \frac{i(a^2 - r^2)}{4\nu} \tag{6.21}$$

From (6.21) we see that not only do a zero in the last factor cancel the pole in the first factor for very low frequencies, but we also regain the Poiseuille-Hagen velocity profile for the flow. This is in accordance with our expectations from a physical point of view. It is now clear that the poles contributing to the residues of eq (6.13) comes only from the Bessel function and from the transform of the pressure functions.

The poles contributed by the Bessel function in eq. (6.8) are

$$J_{0,k} = (a\sqrt{\frac{-i\omega_k}{\nu}}) \Leftrightarrow \omega_k = i\nu\Big(\frac{J_{0,k}}{a}\Big)^2, \tag{6.22}$$

where $J_{0,k}$ refers to the real-valued zeros of a Bessel function of the order zero. As $J_0(z) = J_0(-z)$, we find that the poles contributed by the Bessel function in eq. 6.8 are situated along the entire imaginary axis.

6.3 Calculation of responses

Having considered the general approach towards solving the problem of oscillating flow, and as we have found the poles contributing to the residues,

we will proceed to determine the velocity profiles that occur as a result of the different pressure disturbances exiting the pipe system through the means of viscous effects. From the velocity profiles we find the volume flow through integration. This enables us to express the response of the system as we regard the pressure at the inlet as the input signal and the corresponding volume flow through the pipe system as the output.

$$Q(t) = 2\pi \int_0^a ru(r,t)dr = \pi a^2 \bar{u}(t), \tag{6.23}$$

where $Q(t)$ denotes the corresponding volume flow and $\bar{u}(t)$ denotes the mean velocity through the pipe.

6.3.1 Impulse response

Velocity profile response

The transform of an impulse distribution does not contribute any poles, and as such the only poles contributed to the residue in this case comes from the zeros of the Bessel function. They are of the first order, and as such they can be calculated as follows

$$u(r,t) = \frac{1}{\rho l} \sum_k Res\big[f(\omega)\Delta p, \omega_k\big] = \frac{1}{\rho l} \sum_k \lim_{\omega \to \omega_k} \Delta p f(\omega)(\omega - \omega_k), \tag{6.24}$$

where $\omega_k = i\nu(j_{0,k}/a)^2$.

We will now rewrite the function $f(\omega)$, found in eq. 6.10, as a fraction where only the factor contributing poles are written in the enumerator

$$f(\omega) = \frac{h(\omega)}{g(\omega)} = \frac{\frac{1}{\omega}\left(J_0\big(a\sqrt{\frac{-i\omega}{\nu}}\big) - J_0\big(r\sqrt{\frac{-i\omega}{\nu}}\big)\right)e^{i\omega t}}{J_0\big(a\sqrt{\frac{-i\omega}{\nu}}\big)}. \tag{6.25}$$

Utilizing this we now write eq. 6.24 as

$$u(r,t) = \frac{1}{\rho l} \sum_k \lim_{\omega \to \omega_k} \frac{\Delta p h(\omega)}{\frac{g(\omega)}{(\omega - \omega_k)}} = \frac{\Delta p}{\rho l} \sum_k \frac{h(\omega)}{g'(\omega)}\bigg|_{\omega=\omega_k} \tag{6.26}$$

$$= \sum_k \frac{\Delta p}{\rho l} \left(\frac{\left(J_0\big(a\sqrt{\frac{-i\omega}{\nu}}\big) - J_0\big(r\sqrt{\frac{-i\omega}{\nu}}\big) \right) e^{i\omega t}}{-\omega J_1\big(a\sqrt{\frac{-i\omega}{\nu}}\big)\sqrt{\frac{-ia^2}{4\nu\omega}}} \right) \Bigg|_{\omega=\frac{i\nu j_{0,k}^2}{a^2}}$$

$$= \frac{2\Delta p}{\rho l} \sum_k \frac{1}{j_{o,k}} \left(\frac{J_0\big(\frac{r}{a} j_{o,k}\big)}{J_1\big(j_{o,k}\big)} \right) e^{-\nu(\frac{j_{0,k}}{a})^2 t} = G(r,t). \tag{6.27}$$

Realizing the importance of eq. 6.27, as it represents the impulse response of the system, we will define it as $G(r,t)$. We note that the unit of $G(r,t)$ is $[m/s^2]$ as it is required to be integrated over dt along with an other function. This corresponds to $G(r,t)$ being a Greens function [11], which is a solution to

$$L\{G(r,t-t')\} = \delta(t-t'), \tag{6.28}$$

where

$$L\{\} = \frac{\partial^2}{\partial r^2} + \frac{1}{r}\frac{\partial}{\partial r} + \frac{\rho}{\mu}\frac{\partial}{\partial t}. \tag{6.29}$$

We then have that the velocity profile resulting from any pressure disturbance can be found from

$$L\{u(r,t)\} = \Delta p(t) \tag{6.30}$$

With a solution that can be written as:

$$u(r,t) = u_0(r,t) + \int_{\infty}^{-\infty} G(r,t-t')\Delta p(t')dt', \tag{6.31}$$

which is a solution of the inhomogeneous problem with the stated boundary conditions.

Volume flow response

We will now integrate of the velocity profile of the flow resulting from a disturbance of the pressure at the inlet in form of an impulse. From this we find the impulse response of the system. We note that the response is given with regard to how the volume flow inside the pipe system changes in response to changes of the pressure gradient.

$$Q(t) = 2\pi \int_0^a rG(r,t)dr$$

[11] We here refer to [4] George Arfken 'Mathematical Methods for Physicists'

$$= \frac{4\pi\Delta p}{\rho l}\sum_k \frac{1}{j_{o,k}} e^{-\frac{j_{0,k}}{a}^2 \nu t} \int_0^a r\left(\frac{J_0\left(\frac{r}{a}j_{o,k}\right)}{J_1\left(j_{o,k}\right)}\right) dr.$$

$$= \frac{4\pi\Delta p a^2}{\rho l}\sum_k \frac{1}{j_{o,k}^2} e^{-\frac{j_{0,k}}{a}^2 \nu t}. \tag{6.32}$$

We see that the first term of eq. 6.32 will dominate as it has the largest coefficient and the largest time constant. As such we will here use $\sum_k j_{0,k} \approx 2.5$.

$$Q(t) \approx \Delta p(t)\frac{2a^2}{\rho l} e^{-\frac{6\nu}{a^2}t}. \tag{6.33}$$

In the Laplace domain this transforms to[12]

$$H_p(s) = \frac{Q(s)}{\Delta p(s)} \approx \frac{2a^2}{\rho l}\frac{1}{s+\nu\frac{6}{a^2}} = \frac{a^4/3\mu l}{(a^2/6\nu)s+1}, \tag{6.34}$$

where $H_p(s)$ denotes the volume impulse response of the system in response to pressure changes at the inlet. The amplification of the system is $a^4/3\mu l$ and the time constant is $a^2/6\nu$. We see that they both increase with an increasing diameter of the pipe, and that they both decrease with an increase of viscosity.

From the above we have that the model would predict that we could achieve an arbitrary fast response by decreasing the diameter of the pipe. Here we note that we have not considered the capillary effects. These effects are normally small, but come into play when we are considering fluid moving through very narrow passages. Qualitatively we predict that the capillary and viscous effects can be considered linear, and that the time constant of the capillary effects will increase rapidly as the radius of the pipe becomes very small. Hence, we will reach a point where a decreasing diameter of the pipe will result in a increasing time constant of the system.

Figure 6.2 shows the impulse response of the pipe system. We have chosen the values $\Delta p = 1$ [Pa], $a = 1$ [cm], $l = 10$ [cm] and used the characteristics of air.[13] The response is given in time as the corresponding volume flow following a unit size change of the pressure in form of an impulse. We note

[12] We here refer to [3] B. P. Lathi 'Linear Systems and Signals'

[13] These values will be used further on as both the frequency- and step response are illustrated.

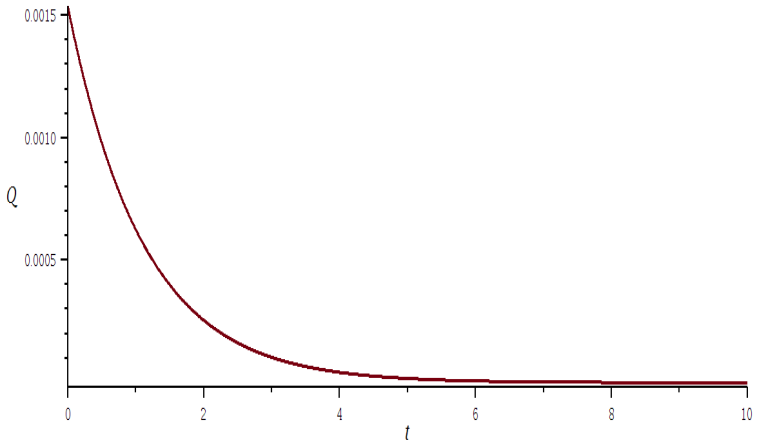

Figure 6.2: Impulse response of the pipe system

how the timescale is of order of seconds.

The viscous forces resulting from a pressure difference in the system acts instantaneously along the entire pipe system, and there is no time delay. This is in contrast to the effects caused by compressibility. Here we must remember that the viscous effects are continuous along the length of the fluid in a laminar flow and as such does do not depend on time. What we are concerned with here is for how long it takes for the corresponding volume flow to adjust to the new conditions, and not for how long it takes for the pressure to propagate.

It would be of much practical interest to model a transfer function for the system connecting the pressure at the inlet to the pressure measured at any point in the pipe system. We here suspect that this transfer function will have an amplification equal to one and a time constant as for the transfer function found in eq.6.34. What is amplified in this thesis is that even as a change in pressure reacts simultaneously in the entire system, the corresponding volume flow takes some time to adjust to the new pressure conditions. It is therefore clear that using an ordinary pressure gauge to measure a fluctuating flow, the gauge will measure the pressure of the volume flow that adjusts according to the time constant of the viscous effects. Hence, we will not acquire the correct pressure reading until the volume flow has had time to adjust to the new pressure conditions.

6.3.2 Frequency response

Velocity profile response

For an harmonic function of a single frequency, for which the transform yields a pole in $\omega_m = \omega_0 + i\epsilon$ in the upper half plane, we have that

$$u(r,t) = \frac{1}{\pi\rho l}\Bigg(\sum_k Res\big[f(\omega)\lim_{\epsilon\to 0}\frac{\Delta p\epsilon}{(\omega-\omega_0)^2+\epsilon^2}, \omega_k\big] + Res\big[f(\omega)\lim_{\epsilon\to 0}\frac{\Delta p\epsilon}{(\omega-\omega_0)^2+\epsilon^2}, \omega_m\big]\Bigg). \tag{6.35}$$

We realize that this is calculated as

$$u(r,t) = \frac{G(r,t)}{\pi\rho l}\lim_{\epsilon\to 0}\sum_k \frac{\epsilon\Delta p}{((\omega-\omega_0)^2-\epsilon^2)}\bigg|_{\omega=i\nu\frac{J_{0,k}^2}{a^2}} + \frac{1}{\pi\rho l}\lim_{\epsilon\to 0}\frac{\epsilon\Delta p}{((\omega-\omega_0)+i\epsilon)\omega}\left(1-\frac{J_0\big(r\sqrt{\frac{-i\omega}{\nu}}\big)}{J_0\big(a\sqrt{\frac{-i\omega}{\nu}}\big)}\right)e^{i\omega t}\bigg|_{\omega=\omega_0+i\epsilon}. \tag{6.36}$$

As the first factor of eq. (6.36) clearly approaches zero in the limit $\epsilon \to 0$, it is sufficient to only consider the last factor as we continue.

$$u(r,t) = \frac{1}{\pi\rho l}\lim_{\epsilon\to 0}\frac{\epsilon\Delta p}{(\omega_0+i\epsilon)((\omega_0+i\epsilon-\omega_0)+i\epsilon)}\left(1-\frac{J_0\big(r\sqrt{\frac{-i(\omega_0+i\epsilon)}{\nu}}\big)}{J_0\big(a\sqrt{\frac{-i(\omega_0+i\epsilon)}{\nu}}\big)}\right)e^{i(\omega_0+i\epsilon)t}$$

$$= \frac{1}{\pi\rho l}\lim_{\epsilon\to 0}\frac{\epsilon\Delta p}{(\omega_0+i\epsilon)(2i\epsilon)}\left(1-\frac{J_0\big(r\sqrt{\frac{-i(\omega_0+i\epsilon)}{\nu}}\big)}{J_0\big(a\sqrt{\frac{-i(\omega_0+i\epsilon)}{\nu}}\big)}\right)e^{i(\omega_0+i\epsilon)t}, \tag{6.37}$$

which yields the solution[14]

$$u(r,t) = \frac{-i\Delta p}{2\pi\rho l\omega_0}\left(1-\frac{J_0\big(r\sqrt{\frac{-i\omega_0}{\nu}}\big)}{J_0\big(a\sqrt{\frac{-i\omega_0}{\nu}}\big)}\right)e^{i\omega_0 t}. \tag{6.38}$$

[14]This result is in accordance to the solution given by Per Amund Amundsen in his unpublished note concerning 'Oscillating flow in a pipe'

Volume flow response

The frequency volume response of the system becomes

$$Q(t) = 2\pi \int_0^a r \frac{-i\Delta p}{2\pi\rho\omega_0 l}\left(1 - \frac{J_0\big(r\sqrt{\frac{-i\omega_0}{\nu}}\big)}{J_0\big(a\sqrt{\frac{-i\omega_0}{\nu}}\big)}\right)e^{i\omega_0 t}dr$$

$$= \frac{-i\Delta p a^2}{16\rho l\omega_0}e^{i\omega_0 t}\left(\frac{J_2(a\sqrt{\frac{-i\omega_0}{\nu}})}{J_0(a\sqrt{\frac{-i\omega_0}{\nu}})}\right). \tag{6.39}$$

Eq. 6.39 represents the frequency response of a pipe filled with fluid as we consider the viscous effects only. As we further define

$$Q(t) = Q_0 e^{iw_0 t} \text{ and } \Delta p(t) = \Delta p_0 e^{iw_0 t}, \tag{6.40}$$

we can express the frequency response as a transfer function relating the pressure and the volume flow in the pipe system[15]

$$H(\omega) = \frac{Q_0}{\Delta p_0} = \Re\left[\frac{-ia^2}{16\rho l\omega}\left(\frac{J_2(a\sqrt{\frac{-i\omega}{\nu}})}{J_0(a\sqrt{\frac{-i\omega}{\nu}})}\right)\right]. \tag{6.41}$$

The real part of eq. 6.41 can be found from the relation $J_n(\sqrt{-i}z) = (-1)^n(ber_n(z) - ibei_n(z))$, where $ber_n(z)$ and $bei_n(z)$ are Kelvin functions[16].

$$H(\omega) = \Re\left[\frac{-i\Delta p a^2}{16\rho l\omega}\left(\frac{ber_2(a\sqrt{\frac{\omega}{\nu}}) - ibei_2(a\sqrt{\frac{\omega}{\nu}})}{ber_0(a\sqrt{\frac{\omega}{\nu}}) - ibei_0(a\sqrt{\frac{\omega}{\nu}})}\right)\right]$$

$$= \frac{\Delta p a^2}{16\rho l\omega}\left(\frac{ber_2(a\sqrt{\frac{\omega}{\nu}})bei_0(a\sqrt{\frac{\omega}{\nu}}) - ber_0(a\sqrt{\frac{\omega}{\nu}})bei_2(a\sqrt{\frac{\omega}{\nu}})}{ber_0^2(a\sqrt{\frac{\omega}{\nu}}) + bei_0^2(a\sqrt{\frac{\omega}{\nu}})}\right). \tag{6.42}$$

We now have that given an input in the form of a harmonically oscillating pressure function the resulting velocity profile in the pipe is

$$\cos(\omega t + \phi) \Rightarrow H(\omega)\cos(\omega t + \phi). \tag{6.43}$$

[15] We here refer to [3] B. P. Lathi 'Linear Systems and Signals'

[16] We here refer to [7] Frank W. Olver, Danile W. Lozier, Ronald F. Boisvert and Charles W. Clark 'Nist handbook of mathematical functions'

It is now clear that we have means to regard the viscous effects of a fluid inside a pipe as a lowpass filter. Figure 6.3 illustrates this by showing the frequency response. We note that figure 6.3 refer to the amplitude response and that there is no face response given the instantaneous reaction in the entire flow caused by the viscous effects. We see that the break frequency is at around $\omega = 1$ [Hz]. This corresponds to the time scale of the impulse response being of the order of seconds. For frequencies over $\omega \approx 10$ we have more or less complete dampening. This means that the pipe system will not have any significant response in volume flow for changes in the pressure occurring over a period of less than the order of tenth of seconds.

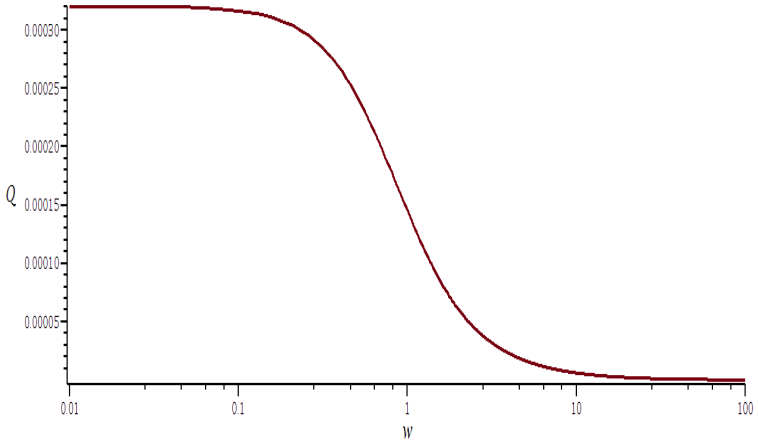

Figure 6.3: Frequency response of a straight pipe filled with fluid.

6.3.3 Step response

Velocity profile response

As we now consider a step distribution lasting for an infinite time. We have a pole in $\omega_m = i\epsilon$. By choosing ϵ to be arbitrary small we can utilize the argumentation made in section 6.2.4, concerning the behavior of $f(\omega)$ at very low frequencies. We will therefore here use $\omega_m \approx 0$ as we write

$$u(r,t) = \frac{1}{\rho l}\left(\sum_k Res\left[f(\omega)\frac{\Delta p}{i\omega}, \omega_k \right] + Res\left[f(\omega)\frac{\Delta p}{i\omega}, \omega_m \right] \right). \qquad (6.44)$$

We substitute eq. 6.27 and eq. 6.21 into eq. 6.44 and as such we have

$$u(r,t) = \sum_k \frac{\Delta p}{i\omega} G(r,t)\bigg|_{w=i\nu\frac{j_{0,k}^2}{a^2}} + \frac{\Delta p}{i} f(0), \tag{6.45}$$

which yields

$$u(r,t) = \Delta p \left(\frac{(a^2-r^2)}{4\rho l \nu} - \frac{2a^2}{\rho l \nu} \sum_k \frac{1}{j_{0,k}^3} \left(\frac{J_0\left(\frac{r}{a} j_{o,k}\right)}{J_1\left(j_{o,k}\right)} \right) e^{-\left(\frac{j_{0,k}}{a}\right)^2 \nu t} \right). \tag{6.46}$$

We now have the transient and everlasting term of the flow resulting from a pressure change in the from of a step described separately in eq. 6.46. We see that as the time t increases the flow approach the Possuille-Hagen profile for the flow as expected.

From a mathematical point of view it is worth noticing that as the flow must be zero at $t = 0$, the two terms making up eq. 6.46 must yield the same value at that instant. Hence, we have by chance found the sum of the Bessel functions zeros when presented as in eq. 6.46. We have that

$$\sum_k j_{0,k} \left(\frac{J_0\left(\frac{r}{a} j_{o,k}\right)}{J_1\left(j_{o,k}\right)} \right) e^{-\left(\frac{j_{0,k}}{a}\right)^2 \nu t} = \frac{(a^2-r^2)}{8a^2}. \tag{6.47}$$

Volume flow response

The step response of the system can be found as

$$\begin{aligned} Q(t) &= 2\pi \left(\int_0^a r \frac{(a^2-r^2)}{4\rho l \nu} dr - \frac{2a^2}{\rho l \nu} \sum_k \frac{1}{j_{0,k}^3} e^{-\left(\frac{j_{0,k}}{a}\right)^2 \nu t} \int_0^a r \left(\frac{J_0\left(\frac{r}{a} j_{o,k}\right)}{J_1\left(j_{o,k}\right)} \right) dr \right. \\ &= 2\pi \left(\frac{a^4}{16\rho l \nu} - \frac{2a^4}{\rho l \nu} \sum_k \frac{1}{j_{0,k}^4} e^{-\left(\frac{j_{0,k}}{a}\right)^2 \nu t} \right) \\ &= \frac{4\pi a^4}{\rho l \nu} \left(\frac{1}{32} - \sum_k \frac{1}{j_{0,k}^4} e^{-\left(\frac{j_{0,k}}{a}\right)^2 \nu t} \right). \end{aligned} \tag{6.48}$$

with $\sum_k j_{0,k} = 2.5$ we have in the Laplace domain

$$\frac{1}{s}H_p(s) \approx \frac{4\pi a^4}{\rho l \nu}\left(\frac{1}{32} - \frac{\frac{a^2}{230\nu}}{\frac{a^2}{6\nu}s + 1}\right). \tag{6.49}$$

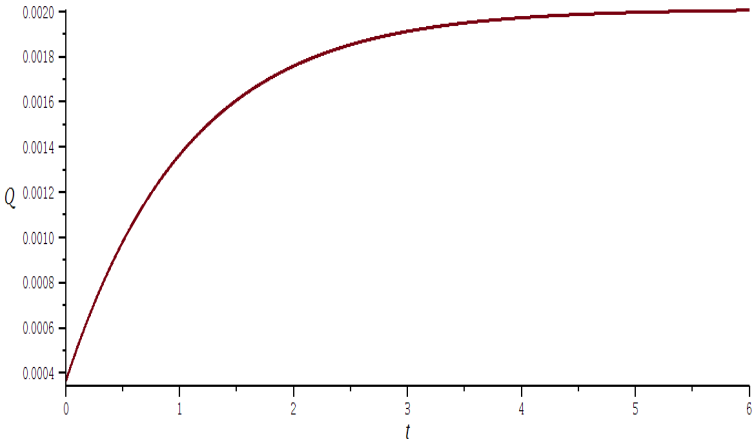

Figure 6.4: Step response of the pipe system.

We see from figure 6.4 that the step response here corresponds with the impulse and frequency response. As we previously have calculated both the impulse and frequency response of the system it might seem excessive to have calculated the step response in addition. We have done this in an attempt to wheel this thesis in the direction of the field of control systems, where the step response is a more common representation of the systems characteristics than the impulse response. Another reason for including the step response is that we during the calculation have stumbled upon a way of finding the sum of the zeros of the Bessel functions. It is unfortunate that there will not be room to pursue this discovery further. If some one where to pick up the trace left behind here it would be interesting to see whether it is possible to find other expressions for the zeros of the Bessel function, or similar functions, by exiting the system to other functions.

Chapter 7

Conclusion

From the above chapters the system can now be described as a circular jet entering a quiescent fluid which after a transition zone can be modeled as a non-viscous flow described by its mean velocity. This we presume remains valid in the contracting part of the pipe system as well as for the two pipes. The above results also demonstrate how the velocity profile and the corresponding volume flow of a stream changes according to changes of the pressure in the pipe system. From this we find the means to express the pipe system as a transfer function. These results also apply to the narrow shaft which the air passes through as some of it leaks out of the pipe system to reach the pressuregauge.

We see that the pressuregauge is not measuring the actual pressure in the pipe system, but the pressure of the corresponding volume flow adjusting to the pressure change in the pipe system. We find that this change occurs over a period of seconds, and that it depends on the maximal radius of the pipe and the viscosity of the fluid. We find that the effects caused by viscosity dominates over the effects caused by compressibility, and as we presume other effects to be even less significant we argue a model of the pipe system based on the viscous effects only.

The entire system, containing both the pipe system and the measuring arrangement, should be regarded as two separate transfer functions in connection. They will both be governed by the same viscous forces, but will have a different diameter of the pipe and hence a different time constant. We have that the time constant of the viscous effects increase with the maximal radius of the pipe in the second order, as such the time constant of the pipe system

will dominate the time constant of the measuring arrangement. Hence, we might discard the time constant associated with the measuring arrangement.

From the frequency response of the system it can be seen that the system acts as a lowpass filter. The viscous forces within the fluid dampens out high frequency changes of the inlet pressure. The physical explanation for this is that the fluid particles takes some time to react to new pressure conditions because of the viscous forces between them. Hence, rapid fluctuations will in an increasing manner be dampened out.

The model of the stationary turbulent flow is mainly an argument for not considering the thickness of the boundary layers under steady conditions. We are reminded that this might not be valid for a fluctuating flow, and that there might be reason for special concern during starting and closing procedures.

It is important to remember that the discussions made in this thesis does not directly apply to the real system under consideration. We have not considered in detail the sonic conditions and effects on the boundary layer that might appear at the inlet of the system. The solution for the jet and the time-dependent solution applies to a laminar flow and we have not considered how to extend these solutions in the case of turbulence and roughness in the pipe that exceeds the hight of the laminar boundary layer. Neither can we be certain to what degree the effects caused by compressibility and turbulence can be regarded as linear with respect to the viscous effects. There are undoubtedly other concerns regarding the model that could have been examined in more detail and we are reminded that this model is to be considered crude.

This thesis has clarified a mathematical model that can be used in the design of an automatic control system that has the ability to regulate the volume flow through the pipe system similar to the one we have discussed here. It should be notes that all the solutions we have arrived at in this thesis is based on pure mathematical and physical assumptions, and that there has been no simulation or testing involved. It could therefore have valuable contributions from computer simulation, such as FEM, and from visualization of the actual phenomena, by for example the means of electrolysis and a transparent pipe.

Chapter 8

References

1. D. J. Tritton; *Physical Fluid Dynamics 2. ed. OPU, Oxford 1988.*

2. Pijush K. Kundu, Ira M. Cohen and David R. Dowling; Fluid Mechanics 5. ed. Elsevier 2012.

3. B. P. Lathi; Linear Systems and Signals 2. ed. Oxford University Press 2010.

4. George Arfken; Mathematical Methods for Physicists 2. ed. Academic Press 1968.

5. Eugen Butkov; Mathematical Physics 1. ed. Addison-Wesley Publishing Company 1968.

6. Per Amund Amundsen; Occilating laminar flow in a pipe. Unpublished note.

7. Frank W. Olver, Danile W. Lozier, Ronald F. Boisvert and Charles W. Clark; Nist handbook of mathematical functions. Cambridge University Press 2010.

8. Maplesoft; Maple 16. Computer program used for some of the calculations and to draw the graphs.